Journal of Geosciences and Geomatics, 2019, Vol. 7, No. 5, 221-236
Available online at http://pubs.sciepub.com/jgg/7/5/2
Published by Science and Education Publishing
DOI:10.12691/jgg-7-5-2

Petrography and Geochemistry of the Somie-Ntem Granitoids (Western Cameroon-Domain): Implication on the Pan-African Evolution of the Central African Fold Belt

Mero Yannah[1,2,*], Juliana Amboh Tifang[2], Eric Martial Fozing[1], Yaya Fodoué[3], Armand Dongmo Kagou[1], Samuel Ndonyui Ayonghe[4]

[1]Department of Earth Sciences, University of Dschang, Dschang, Cameroon
[2]Remote Sensing Unit, Institute of Geological and Mining Research, Yaounde, Cameroon
[3]Research Center for Geology and Mining, Institute of Geological and Mining Research, Garoua, Cameroon
[4]Central Unit for Internal Control and Evaluation, University of Buea, Buea, Cameroon
*Corresponding author: merotumi@gmail.com

Received September 19, 2019; Revised November 12, 2019; Accepted November 24, 2019

Abstract Somie-Ntem area within the Tikar plain form part of the Western Cameroon Domain (WCD) that belong to the Central African Pan-African Fold Belt (CAPFB). Petrography and whole rock geochemistry characterize the granitoids of this area into granites (Gr), granodiorites (GD) and tonalite (Tn) forming group I granitoids. These rocks displaying high-calc-alkaline to shoshonite affinity and strongly metaluminous I-type. They also show strong enrichment in Ba-Sr and no pronounced Euanomaly, belongs to syn-to post collisional tectonic setting. Group II rocks consist of AGr show strange characteristics with high K-calc-alkaline affinity, metaluminous and peraluminous of I-type, and also very poor in Ba-Sr, strong negative Eu anomaly typical of post orogenic. Both groups depleted in Nb, Th, Ti with Pb and Dy enrichment. However, the Al_2O_3/TiO_2vs TiO_2Harker plot show that the group I granitoids originated from a common melt and got differentiated through fractional crystallization during syn-to-post tectonic regime at subduction environment induced by a crustal thickening tectonic regime. Group II granitoids are post orogenic, emplaced following tectonic extension at subduction leading to the injection of strongly evolved magma from partial melting of new material at the lower crust.

Keywords: *granitoids, petrography, geochemistry, somie-ntem, tikar plain, pan-african, cameroon*

Cite This Article: Mero Yannah, Juliana Amboh Tifang, Eric Martial Fozing, Yaya Fodoué, Armand Dongmo Kagou, and Samuel Ndonyui Ayonghe, "Petrography and Geochemistry of the Somie-Ntem Granitoids (Western Cameroon-Domain): Implication on the Pan-African Evolution of the Central African Fold Belt." *Journal of Geosciences and Geomatics*, vol.7, no. 5 (2019): 221-236. doi: 10.12691/jgg-7-5-2.

1. Introduction

Tectonism and orogenic processes are often characterized by the emplacement of granitoid intrusions during and after these events. These granitoids usually carry geochemical information that gives indications on collisional magmatic processes within the continental lithosphere and their contribution to the intra-crustal recycling of the continental crust together with the constraint on the tectonic environment [1]. The study area is found (Figure 1) on the western part of the Central Cameroon Shear Zone (CCSZ, [2,3]) and on the south western margin of the Tcholliré-Banyo Shear Zone [4]. This area crosscut the segment of Somie in the Adamawa to Ntem in the North West region of Cameroon, forming the north western margin of the Tikar Plain. It belongs to a chain of alkaline complexes that characterized the Tikar plain in particular [5] and the Central African Orogenic Belt (CAOB) in general. The Pan-African lithologies previously identified as Late Neoproterozoic [6] are known to span from Cameroon through Chad to the Central African Republic before reaching the Republic of Congo and North East of Nigeria [7] and forming a huge part of the Central African Orogenic Belt (CAOB). However, Pan-African granitoids occur vastly within the CCSZ, described by many authors as syn-to-post collisional, calc-alkaline, ferro-potassic, metaluminous to weakly Peraluminous [4,8-16]. Nevertheless, granitoids of the Somie-Ntem segment of the Tikar plain have not been studies yet aside from studies in some of the massifs around the area [5,17]. The petrography and geochemistry characteristics of granitoids in this area will enable an appraisal of the tectonic relationship that exist between the Somi-Ntem area and the Pan-African orogeny. This shall take into consideration the determination of: 1) their source and (2) discuss their implication to the Pan-African evolution of the Central African Fold Belt (CAFB).

2. Regional Geological Setting

2.1. The Pan-African and the CCSZ

The Pan-African orogeny forms the Central African orogenic belt of Late Neoproterozoic [6] and a product of the collision of the São Francisco Craton, the Congo Craton, and the West African Craton during the formation of Gondwana [18,19]. The CCSZ stretches from Cameroon through Chad, north of the Congo Craton, to the southern and the western Nigerian Shield to the north where it continues to the west into the Borborema Province of NE Brazil hosting Brasiliano-Pan-African Granitoids [7]. The Tikar plain falls within the West Cameroon Domain [19] of the Cameroon Orogenic Belt which is characterized by Paleoproterozoic (basement gneisses, migmatites and granulites), Meso -to Neoproterozoic deformed to metamorphosed volcano-sedimentary sequences and the Pan-African granitoids which intruded the former two units [15]. These Pan-African granitoids extend south of the Tchollire- Banyo Fault (TBF) that cuts through Bertouaand extends into the Central African Republic and Chad [20]. According to [15], the Pan-African granitoid emplacement are generally controlled by N30°E strike-slip shear zone that forms a prolongation of the CVL and also by the N70°E Central Cameroon Shear Zone (CCSZ). Even though very little has been done in the investigation of the Pan-African granitoids within the CCSZ, [4] differentiated three types of granitoids in relation to deformation within the Pan-African. Such include Pre- to syn-D_1 granitoids, Syn- to post-D_2 granitoids and post-orogenic granitoids [4]. In the petrography study [21] identified four types of granitoids within the CCSZ including: the biotite granitoids, deformed granitoids, mega-feldspars granitoids and two mica granitoids. The emplacement of these Pan-African granitoids took place at the early stage of tectonic deformation forming the orthogneisses [4] that cuts through the Cameroon fold belt. Rocks of the Tikar plain mostly include the calc-alkaline metadiorites to granodiorites belonging to Pre-to Syn D_1 and found mostly west of the Tchollire´-Banyo fault. Studies on some of these granitoids indicate the presence of hornblende-biotite granitoids, biotite±muscovite granitoids and the biotite granitoids [20]. Different methods have been used to date the Pan-African granitoids in Cameroon and Nigeria including: Rb-Sr whole rock of the Godé granite giving 545± Ma [22], the Tchembametadiorite using U-Pb in zircon giving age of 633±3 Ma [23] and the hornblende/biotite granites of Rahama using Ar-Ar method gave 565±5 Ma [24]. In general, Pb-Sr whole-rock and Th-U-Pb ages on monazite (CHIME method) gave emplacement ages for these granitoids varying between 609 ± 30 Ma and 510 ± 8 Ma [14,25].

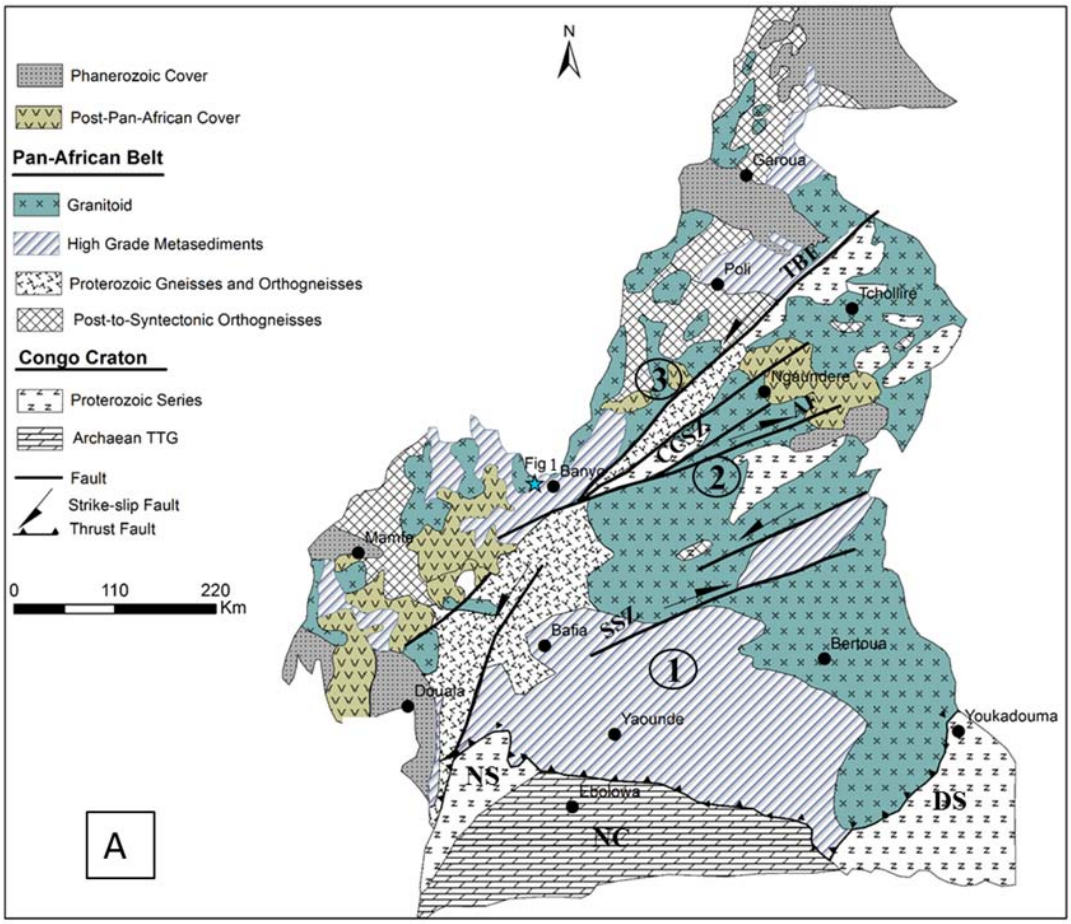

Figure 1. The Cameroon geologic map showing the major lithotectonic units [4,73];:***NS***-Nyong Series, ***NC***-Ntem Complex, ***DS***-Dja Series; different domains of rock suite [19]: **1**-Yaounde Domain (YD), **2**-Adamawa-Yadé domain (AYD), **3**-West Cameroon Domain (WCD), ***AF***-Adamawa fault; major faults and shear zone [2,4]: ***TBF***-Tcholliré-Banyo fault; ***SF***-Sanaga fault; ***CCSZ***-Cantral Cameroon Shear Zone, ***SSZ***-Sanaga Shear Zone, Figure 1 label (star) represent the study area

2.2. Geology of the Study Area and CCSZ

The study area is characterized by Pan-African granitoids (Figure 1) occurring in association with Post-Pan-African plutons with a Pre-to-syn tectonic magmatic gneissic basement [4] partly covered by volcanic rhyolites. Several authors have worked in the study area [26,27,28] and identified rocks of the Tikar plain to vary from low basic through intermediate acid rocks with SiO_2-undersaturated. Other reports show that the Pan-African intrusions including the Tikar Plain display a spatial relationship with the CCSZ characterized by a dominant N70°E orientation [29]. Studies on some of the complexes and massifs of the Tikar plain show lithological relationship between the volcanic and the plutonic units occurring in close association in what was described as plutonic-volcanic complexes [30]. The Pandé massif east of the plain contains coarse-fine grained syenite-granites, granites (plutonic unit) and trachyite-rhyolites and rhyolite (volcanic unit) intruding the Pan-African granite basement [17]. Meanwhile, the Sabongari complex consist of granites, syenites, micro and monzodiorite as the plutonic rock assembly while basalts, trachytes and rhyolites defines the volcanic counterparts [5]. The pre-tectonic association of these granitoids in relation to the aluminum saturation place them generally within the metaluminous-peralkaline (basic group) and metaluminous-peraluminous (felsic group) compositions [5]. A comparative appraisal of the Tikar plain complexes show that the Mbafé, Pandé and Pamsa unlike the Sabongari complex are poor in their petrographic variability as most of the rocks are felsic with few basic varieties [31]. Another significant difference includes the mineralogy between the Pande and the Sabongari complexes characterized by the occurrence of sodic pyroxene (aegerine) and amphibole (arfvedsonite) within the syenites [17]. The Mbakop complex situated south west of the Sabongari, occur as a N-S elongated granitoid composed of deformed biotite and hornblende granites emplaced within biotite gneisses and amphibolites [3]. These Mbakop gneisses are rich in biotite, quartz, plagioclases and k-feldspars porphyroclast with magnetite, hematite, sphene, apatite and epidote as accessory mineral components [3]. The mineral assemblages made up of sphene + apatite + oxides + quartz + alkali feldspars, to plagioclases + biotite ± amphibole ± pyroxene ± zircon occur within the ortho and parageneticprotomylonites that defined the Foumban-Bankim branch of the CCSZ [32]. This study provides new petro-geochemical data of the Somie-Ntem transect, western margin of the Tikar plain.

3. Sampling and Analytical Procedure

Petrographic study made use of thirty thin sections produced at the Laboratory of the University of Johannesburg, South Africa. The thin sections were observed using x2.5 objective of the Optika vision light petrographic microscope at the Institute of Geological and Mining Research Yaounde Cameroon. Geochemical samples for this study were collected with focus on compositional changes within the rocks to increase the possibility of knowing the exact chemical composition of the rock. Samples pre-preparation took place at the ore laboratory of the Institute of Geological and Mining Research (IRGM) Yaounde Cameroon. At this laboratory, the samples were cut into cube sizes of $5cm^2$ submitted to the Activation Laboratories of Ontario Canada. At the ActLabs, each sample was entirely crushed to a nominal -2 mm, mechanically split to obtain a representative sample and then 250 g of the pulverized rock was brought to 95% -105 µm. The powders were then inserted into the Inductive Coupled Plasma Mass Spectrometer (ICP-MS) for analysis. The analytical method known as 4Litho is a method that combines the whole rock ICP-OES and trace elements ICP-MS packages in a Lithium Metaborate/Tetraborate Fusion - ICP and ICP/MS. Here, fused sample gets diluted and analyzed by Perkin Elmer Sciex ELAN 6000, 6100 or 9000 ICP-MS. Three blanks and five controls (three before sample group and two after) were analyzed per group of samples. Duplicates were fused and analyzed every 15 samples. Instrument was recalibrated after every 40 samples analyzed. The detection limits for the major elements were set at 0.01 % except for MnO and TiO_2 with 0.001 %. The trace elements except for Zn with 30 ppm, Ni and Cr with 20 ppm, Pb, As and V with 5 ppm the rest of the elements have detection limits of≤ 2 ppm. Data analysis followed geochemical classification by [33] using multi-cationic methodfor igneous rocks while trace elements normalization and plotting was done following the system [34,35]. Aluminium and silica saturation was determined using method by [36,37].

4.Results

4.1. Petrography

The study area is characterized by different types of granitoids made up of granites (Gr), alkali-granites (AGr), granodiorites (GD) andtonalite (Tn). These plutonic rocks form over 60 % of rocks in the study area (Figure 2) and are hosted by shades of migmatitic gneisses with partial volcanic cover as rhyolites. These granitoids outcrop mostlyonthe north and north western part of the study area, displaying a predominant NE-SW and slightly E-W orientation.

4.1.1. Granites (Gr)

Gr occur as the most abundant granitoids, outcropped along the western margin of the Somie-Ntem stretch, forming elongate plutons (Figure 3a& Figure 3ai) and tors (stacked boulders). Field texture vary from aplitic to porphyritic with inclusions of the porphyritic texture common within the finer grained variety. The micro fabric show inequigranular texture, intergranular and intragranular micro fractures crosscutting the feldspars and quartz grains with the mineralogy made up of orthoclase 40-45 vol %; quartz with 25-30 vol %, plagioclase 5-10 vol %, the mafic group varies from 2-5vol % made up principally of biotite. The accessory phase constitute about 3-5 vol % including titanite, zircon and iron oxide. Quartz show anhedral grains 0.1 to 0.1 mm large and up to 1 mm in the porphyritic varieties with irregular margins. Plagioclase shows inequigranular subhedral to anhedral texture,

displays flame perthiteand myrmekites structures and deformation lamellae with grain size varying from 0.03-1 mm. Orthoclase generally display euhedral to anhedral inequigranular in texture, show Carlsbad twining, bear intragranular fractures and display moderate to intense sericitization.Biotite occurs as dark brown, lath-like crystals wrapped around the feldspars and quartz grains. The accessory zircon, titanite, and iron oxide form inclusions within the biotite bearing granites while iron oxide and titanite occupy mostly the grain boundaries.

4.1.2. Alkali granite (AGr)

AGr display medium-coarse-grained, homogenous inequigranular texture, greyish-white color and generally phaneritic. Individual crystals of the felsic minerals bear intragranular fractures. Mineralogical composition include: quartz, plagioclase and orthoclase with 50 - 55vol %, 5 - 10 vol % and 40 - 45 vol % and respectively. The mafic constituents consist of hornblende and clinopyroxene making up 10 - 20vol % of the rock. The accessory and secondary minerals make up 3 - 5 vol % including titanite, zircon, iron oxide and quartz (Figure 3 b). Micro fabric show quartz with euhedral to anhedral crystal, grainsize vary from 0.3 to 1 cm large,showing interconnection with plagioclase and orthoclase. Quartz aggregate locally occur at grain boundaries while intergrowth of secondary quartz and orthoclase develop intense granophyric texture in the (Figure 3 bi & Figure 3 bii). Sericitizationsilicificationis moderate to intense in the rock and mostly attack the plagioclase and orthoclase. Most often, only the twin plane are visible. Orthoclase and plagioclase crystal vary from 0.06 - 1 com, locally bear iron oxide, titanite zircon inclusions. Hornblende and clinopyroxene crystals occur mainly as single, skeletal grains measuring 0.03 - 0.5 cm and locally display perthite exsolution and xenomorphic structure.

4.1.3. Granodiorites (GD)

GD show dark grey color with coarse-grained texture (Figure 4a). The mineral constituent is dominated by quartz and plagioclasemaking 40-45 vol % and 20-30 vol % respectively. K-feldspar constitutes 10-15 vol % of the rock. The mafic constituents consist of biotite with some hornblende making 10-15 vol % of the rock. The accessory and secondary minerals make up 2-5 vol % including titanite, iron oxide, zircon and chlorite. Both orthoclase and plagioclases in these rocks show subhedral crystals with grain size from 0.1-1 mm, making contact with biotite and feldspars with intense sericitization (Figure 4ai). Anhedral quartz often occupies the T-junctions and grain boundaries alongside the accessory minerals. Biotite is generally subhedral lath-like to skeletal texture, occupying mineral interstices, show string sericitization and locally chloritized with grain size <1 mm. In general, sericitization in this rock affects grain boundaries within grain and the micro-fracture lines.

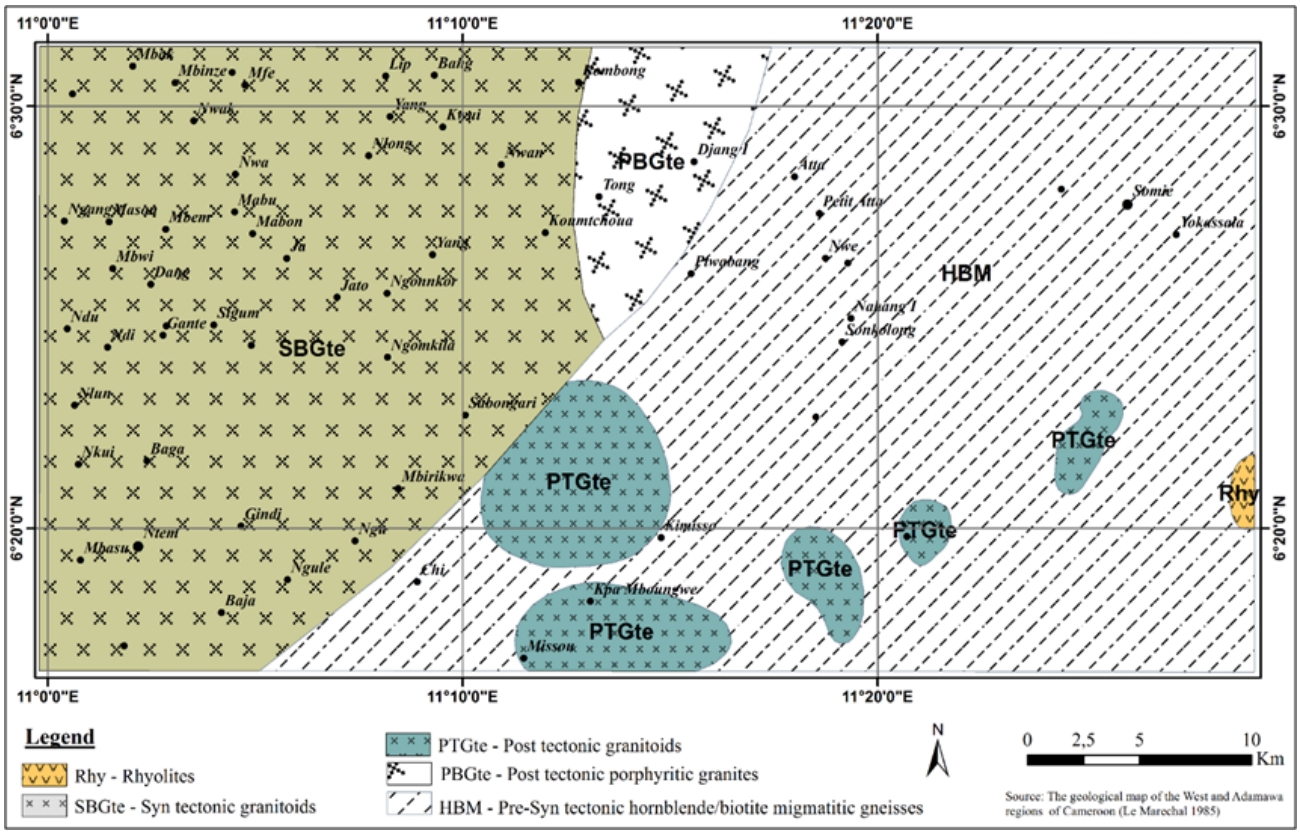

Figure 2. Geological map of the Somie-Ntem, extract from the north western margin of the Tikar plain after [38] showing the main lithological units within the study area, SBGte-Syntectonic-calc-alkaline granites, PTGte-post tectonic granites, Rhy-rhyolites, HBM-hornblende-biotite gneisses, PGte-porphyritic granites

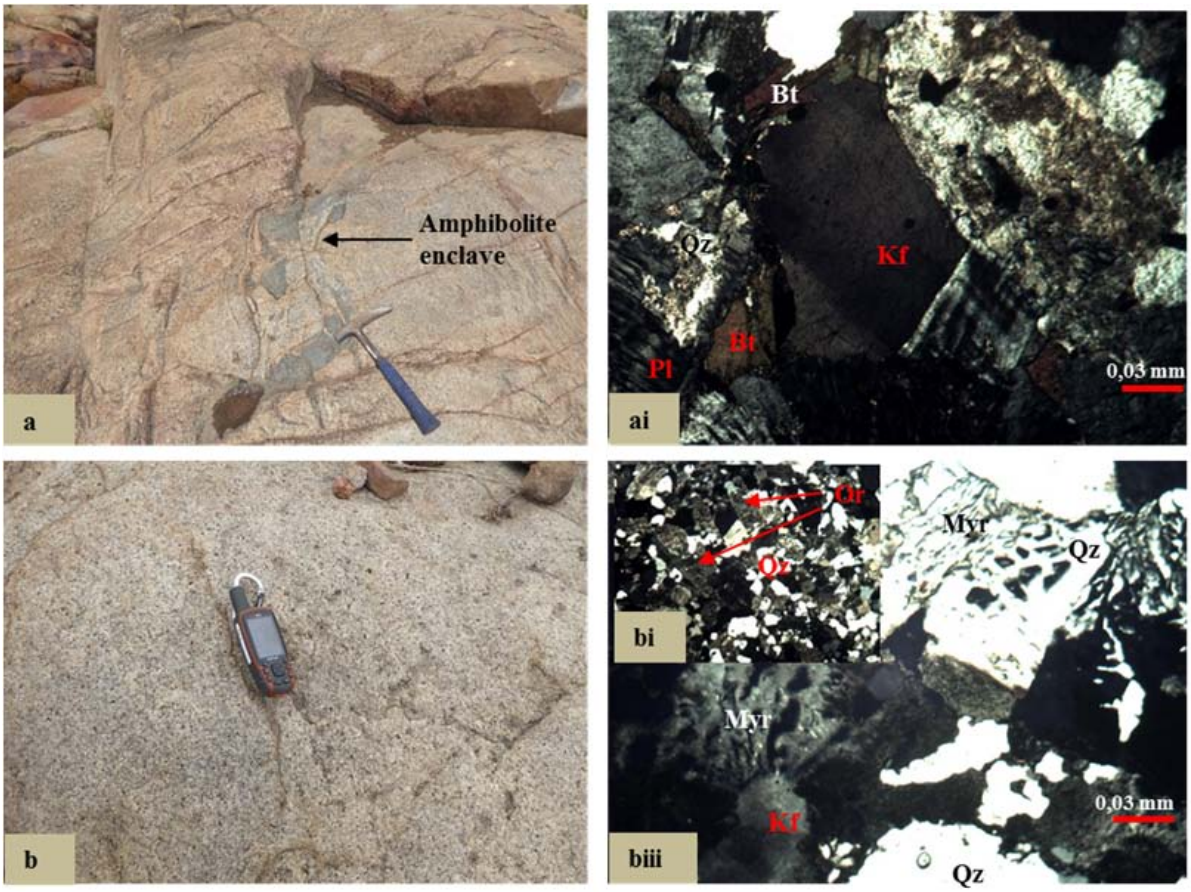

Figure 3. Field and photomicrographs of Granitoids (x2.5 magnification under cross polar); (ai&aii) graniteshowingdeformed amphibolite enclave during granite crystallization; (b, bi&bii) alkali granites with thin section showing intense Myr-myrmekitization and graphic texture.

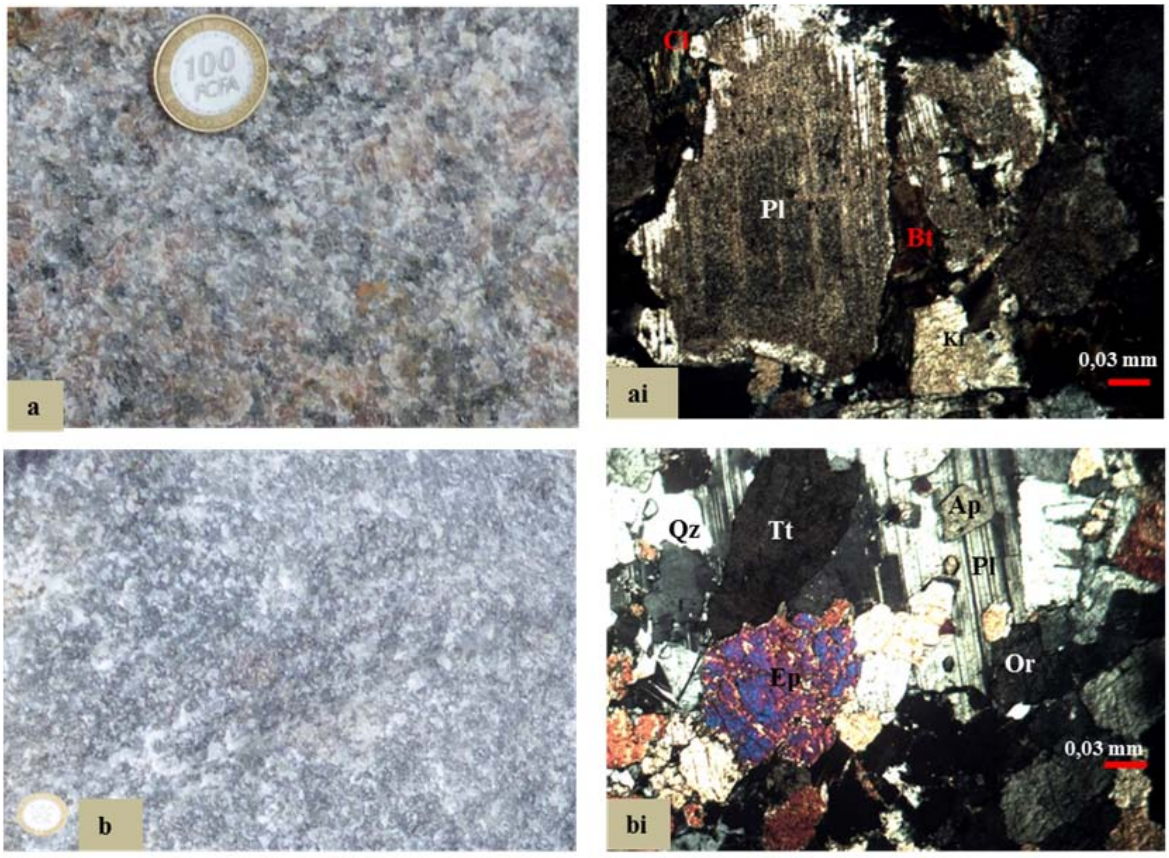

Figure 4. Rock samples and photomicrographs of granitoids; (a &ai) granodiorite withCl-chlorite and sericite alteration (b &bii) tonalite showing poikilitic Pl-plagioclasecrystal bearing AP-apatite, Qz-quartz, Ep-epidote and Ti-titanite inclusions.

4.1.4.Tonalite(Tn)

Tn occurs as massive rock, medium-to-coarse-grained with dark-grey color (Figure 4 b) outcrop in association with GD and Gr Rocks composed of quartz 25-30 vol %, orthoclase10 - 15vol %, microcline 3 – 5 vol %, plagioclase 30 - 35vol %, biotite 10-15 vol %, amphibole 2- 5vol %, epidote5 - 10vol %, while the accessory phases made of apatite, zircon, titanite opaque minerals making 3-5 vol % of the rock. Quartz show anhedral sub-rounded to elongated crystals (< 1mm long) and as aggregates along grain boundaries (Figure 4 bi). Plagioclase feldspars (0.1 to 2 mm long) commonlydisplay poikilitic texture, perfect flame perthite exsolution and develop myrmekites at feldspars grain boundaries. Orthoclase show anhedral grains with embayed margins, forming kink-structures (Figure 4 b ii) and often in contact with quartz, grain size < 1 mm and show intense sericitization. Microcline display subhedral to anhedral crystals with a characteristic tartan twining. The grain size vary from 0.06 – 0.5 mm and commonlypoikilitic. Biotite and amphibole occur at grain interstices together withepidote Accessory mineral form inclusions in the feldspars and biotite.

4.2.Geochemistry

4.2.1. Classification

Geochemical results show the variation in the composition of the Somie-Ntemgranitoids from whole rock geochemistry. The nomenclature for these granitoids according to [33] indicates the presence of plutonic rocks biotite granites, alkali granites, granodiorites and tonalite (Figure 5). Biotite granites are the most common in the area followed by the alkali granite, granodiorites and tonalite.

4.2.2. Major and Trace Elements

The major and trace element content characterize the rock samples of the Somie-Ntem granitoids show group I (Gr, GD and Tn) and group II granitoids (AGr) with variation in geochemical composition.Group I are high in silica content with SiO2 that vary from 64.97-76.35 wt %, Al2O3 = 12.9-16.02 wt %, and Fe_2O_3(T) = 0.56-3.98 wt %. The MgO is low ranging from 0.03-1.54 wt %, P2O5 = 0.08-0.31 wt % and TiO_2 = 0.07-0.73 wt % (Table 1). Meanwhile, the CaO, Na_2O and K2O vary from 1.18-5.3 wt %, 3.25-4.45 wt % and 2.44-6.45 wt % respectively. These granitoids have variable Mg# = 1.15-9.07, K_2O+Na_2O = 7.45-9.07 and the $Al_2O_3/(CaO+Na_2O+K_2O)$ = 1.03-1.54. The trace element content of these granitoids also shows variation amongst the two granitoids groups. The Light Ionic Lithophile Elements (LILE) enrichment over the light with Ba=677-2592 ppm, Rb = 90-224 ppm and Sr = 337-834 ppm (Table 1). High Field Strength Elements (HFSE) on the other hand show depletion with Nb = 6.25 ppm, Zr = 14-428 ppm, Hf = 0.4-10.6 ppm and Ta = 1.3-5.8 ppm. Similarly, the group I Light Rare Earth Elements (LREE) show high fractionation over the Heavy Rare Earth Elements (HREE) with $(La/Lu)_N$ = 10.67-69.95 and $(Gd/Lu)_N$ = 1.37-4.22. Their Eu content show no pronounced negative anomaly but some samples show slight positive anomaly with values from $(Eu/Eu^*)_N$ = 0.6-1.37 (Figure 6). The also show low Rb/Sr ratio from 0.16-0.56, Ba/Rb = 4.62-12.58 and K/Ba = 5.48-66.77. In general, the group I samples show negative anomalies in Nb, P, Ti and a positive Pb and Dy anomalies.

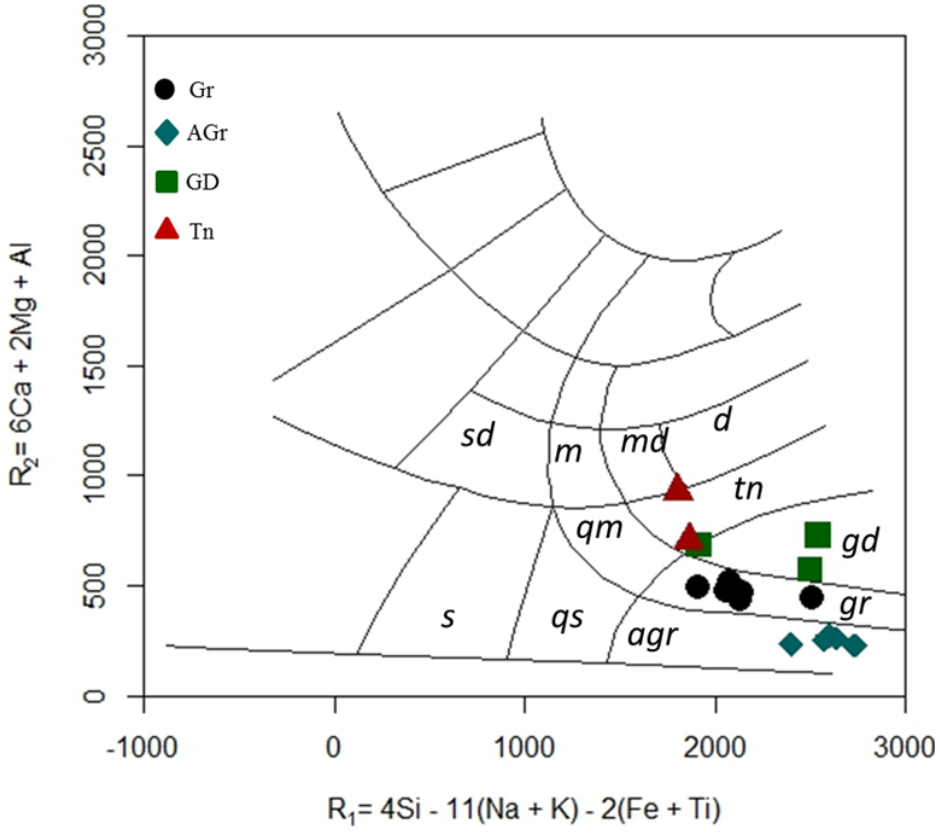

Figure 5. R_1-R_2 multi-cationic classification diagram for igneous rocks [33]; ***tn***-tonalite; ***gd***-granodiorite; ***d***-diorite, ***md***-monzo-diorite; ***gr***-granite; ***qm***-quartz monzonite; ***sq***-quartz syenite; ***sd***-*syeno-diorite*, ***s***-syenite, ***agr***-alkali granite.

Table 1. Major (wt %) and trace (ppm) element compositions of the Somie-Ntem granitoids

Rock Type	Granite						Alkali granite					Granodiorite			Tonalite	
Sample ID	T115-2	T116-1	T121	T122	T127	T136	T120-2	T137	T143	T144	T145	T107-2	T118-2	T177	T107-1	T118-1
SiO_2	68.89	71.19	69.03	69.62	69.55	72.87	75.44	76.35	75.69	75.69	76.35	69.26	71.13	69.57	65.7	64.97
TiO_2	0.546	0.425	0.547	0.491	0.5	0.279	0.035	0.167	0.16	0.16	0.073	0.401	0.349	0.397	0.64	0.725
Al_2O_3	14.77	14.34	14.37	14.77	14.34	13.35	12.9	12.09	11.26	11.26	12.28	14.82	14.35	15.48	14.45	16.02
Fe_2O_3(T)	2.89	2.45	2.96	2.84	2.73	2.08	0.56	1.95	3.16	3.16	1.07	1.96	2.1	3.19	3.36	3.98
MnO	0.036	0.041	0.049	0.047	0.042	0.029	0.009	0.03	0.041	0.041	0.016	0.087	0.047	0.052	0.142	0.066
MgO	0.69	0.56	0.64	0.86	0.57	0.44	0.03	0.03	< 0.01	< 0.01	0.03	0.7	0.45	1.24	1.54	1.5
CaO	1.58	1.18	1.53	1.72	1.48	1.5	0.17	0.11	0.12	0.12	0.17	3.34	2.5	3.38	5.3	2.98
Na_2O	3.25	3.41	3.27	3.82	3.39	3.67	3.44	3.88	4.36	4.36	3.82	4.48	4	4.25	4.25	4.11
K_2O	6.45	5.94	5.83	5.11	5.45	4.4	5.15	4.83	4.66	4.66	4.66	4.69	3.45	2.44	4.48	4.23
P_2O_5	0.17	0.13	0.17	0.2	0.17	0.08	0.01	< 0.01	< 0.01	< 0.01	< 0.01	0.22	0.1	0.11	0.16	0.31
LOI	0.81	0.72	0.55	0.55	0.51	0.37	0.45	0.64	0.4	0.4	0.49	0.52	0.66	0.45	0.36	1.16
Total	100.1	100.4	98.96	100	98.74	99.07	98.2	100.1	99.86	99.86	98.96	100.5	99.14	100.6	100.4	100
Mg#	4.94	4.74	4.49	6.18	4.35	4.4	1.15	0.33	0.01	0.61	0.21	7.21	4.45	7.8	9.07	7.58
Ba	2592	1655	2110	1631	1769	939	896	79	57	15	34	1505	1278	677	1116	1856
Be	2	3	3	5	4	4	2	5	6	6	6	6	5	3	5	4
Co	4	4	4	5	3	4	< 1	1	< 1	1	1	2	3	7	6	8
Cr	< 20	60	80	< 20	60	< 20	< 20	70	90	< 20	110	90	80	130	< 20	20
Cs	1.9	1.4	8.2	8	4.5	2.3	2.3	0.6	0.6	2.3	0.7	2.4	2.9	6.9	1.9	2
Cu	20	20	10	20	< 10	50	< 10	< 10	< 10	< 10	< 10	20	20	10	30	10
Ga	24	22	22	23	21	20	18	37	37	30	38	18	28	18	17	24
Ge	1	1	1	1	1	1	< 1	2	2	2	2	2	1	1	2	1
Hf	10.6	7.3	9.3	6.2	6.4	4.3	0.4	13.8	20.4	5.7	29.8	2.3	6.1	3.3	1.6	7.5
Mo	< 2	< 2	< 2	< 2	< 2	< 2	< 2	3	2	< 2	3	< 2	2	< 2	2	< 2
Nb	10	9	13	10	8	8	< 1	37	56	35	73	11	12	6	25	12
Ni	< 20	< 20	< 20	< 20	< 20	< 20	< 20	< 20	< 20	< 20	< 20	< 20	< 20	< 20	< 20	< 20
Pb	29	40	33	31	27	30	21	9	19	10	18	23	29	17	23	26
Rb	206	224	218	204	222	120	194	155	153	261	173	138	128	90	115	157
Sc	3	3	4	4	3	2	< 1	1	< 1	< 1	< 1	7	6	8	22	7
Sn	4	3	3	2	3	2	< 1	4	9	6	12	2	2	1	3	2
Sr	834	566	727	681	609	563	346	9	4	4	4	472	822	577	337	924
Th	38.9	42.8	34.3	20.7	37.7	55.1	10.9	14.8	18.8	27.3	20	19.2	14.3	11.7	7	19.3
Ta	1.3	1.6	1.9	1.5	1.3	2.4	< 0.1	4	5.8	5	7.6	2.3	1.8	0.8	5.8	1.7
Tl	1	1	1	0.8	1	0.5	0.8	0.5	0.5	0.7	1	0.6	0.5	0.4	0.6	0.8
U	2.2	5.3	3.5	7.1	3.6	16.3	1.8	3.4	4.6	6.8	4.6	2.4	4.7	3.1	2.6	4
V	33	29	31	36	32	21	8	< 5	< 5	< 5	< 5	22	30	51	46	60
W	< 1	< 1	2	2	1	< 1	< 1	1	< 1	3	3	< 1	1	< 1	< 1	< 1
Y	17	17	26	27	14	15	1	63	115	20	49	28	23	8	67	19
Zn	80	50	60	70	60	30	< 30	110	260	< 30	150	90	40	40	100	70
Zr	428	282	389	259	280	161	14	558	906	116	1261	91	261	132	57	326
La	37.3	125	136	75.3	87.8	108	7.3	62.5	79.1	200	44	125	34.6	23.6	37.3	155
Ce	91.1	179	264	178	171	211	12.9	107	162	292	75.8	179	84.6	46.2	91.1	298
Pr	14.5	19.7	28.6	17.8	17.8	21.4	1.19	16.1	17.8	53.2	9.31	19.7	10.3	5	14.5	30.5
Nd	57.6	62.1	95.4	62.5	57.8	67.2	3.6	61.2	62.7	195	29.4	62.1	41.3	16.6	57.6	97.5
Sm	12.7	9.3	14.1	10.6	8.8	10.5	0.5	13	9.8	43	5.7	9.3	7.3	2.9	12.7	14.2
Eu	2.03	1.67	2.17	2.05	1.55	1.66	0.2	0.5	1.96	2.37	0.13	1.67	1.61	0.83	2.03	2.31
Gd	11.4	6.2	8.7	7.2	5.1	5.9	0.4	12.6	6.2	34.4	4.3	6.2	5.4	2	11.4	7.5
Tb	1.9	0.9	1.1	1	0.6	0.7	< 0.1	2.2	0.8	4.9	0.8	0.9	0.8	0.3	1.9	0.8
Dy	11.5	4.8	5.4	5.2	3	3.6	0.2	12.6	3.9	25.5	4.4	4.8	4.3	1.5	11.5	4
Ho	2.3	1	1	1	0.5	0.7	< 0.1	2.4	0.7	4.3	0.9	1	0.8	0.3	2.3	0.6
Er	6.9	2.9	2.8	2.9	1.9	1.4	0.1	6.8	2.1	11.4	2.6	2.9	2.4	0.9	6.9	1.8
Tm	1.03	0.45	0.41	0.45	0.27	0.2	< 0.05	1.04	0.31	1.51	0.38	0.45	0.35	0.13	1.03	0.25
Yb	6.9	3.2	2.5	2.8	1.6	1.2	0.1	6.3	1.9	9.4	2.4	3.2	2.2	0.8	6.9	1.5
Lu	1.03	0.53	0.34	0.43	0.24	0.18	0.01	0.99	0.29	1.34	0.33	0.53	0.37	0.12	1.03	0.22
∑REE	658.82	475.2	625.38	420.52	396.69	391.19	28.57	439.8	185.83	227.82	377.72	392.44	245.84	120.91	120.91	492.12
(La/Yb)N	69.95	45.81	36.87	18.24	28.21	49.6	49.1	6.72	13.44	12.43	3.66	3.66	10.67	19.96	19.96	26.47
(La/Sm)N	6.85	6.45	6.05	4.46	5.06	6.26	9.12	3.02	3.98	4.84	5.53	1.84	2.97	5.1	5.1	8.43
(La/Lu)N	73.22	46.79	41.67	18.24	28.43	50.82	73.64	6.57	14.35	13.87	3.7	3.77	9.74	20.45	20.45	24.55
(Eu/Eu*)N	0.68	0.65	0.6	0.72	0.77	0.71	1.37	0.12	0.6	0.08	0.14	0.52	0.78	1.05	1.05	0.67
(Gd/Lu)N	4.22	3.04	3.17	2.08	2.65	3.51	4.79	1.58	1.94	1.61	0.51	1.37	1.81	2.06	2.06	1.45
(Gd/Yb)N	4.03	2.98	2.81	2.08	2.63	3.43	3.19	1.61	1.82	1.45	0.5	1.33	1.98	2.01	2.01	1.56
(Nb/Ta)	7.69	5.63	6.84	6.67	7.06	6.15	NA	9.25	3.33	7	9.61	4.31	6.67	7.5	7.5	4.78
(Rb/Sr)	0.25	0.4	0.3	0.3	0.17	0.36	0.56	17.22	0.21	65.25	43.25	0.34	0.16	0.16	0.16	0.29

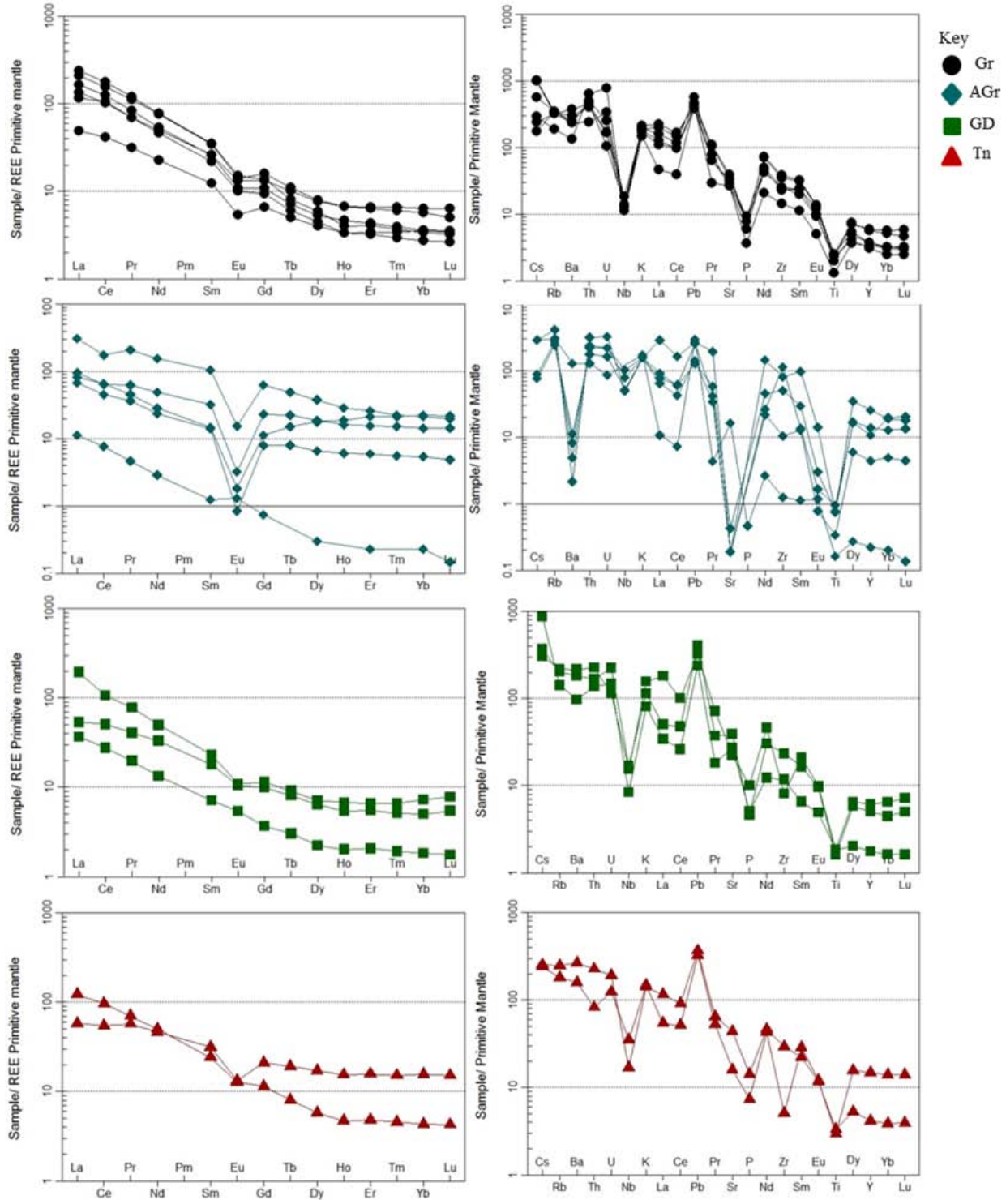

Figure 6. Spidergram of REE patterns for the Somie-Ntem segment granitoids; chondrite normalization of [34,35]

Group II rocks contain very high SiO_2 content ranging from 75.44-76.39 wt %, Al_2O_3 = 11.26-12.90 wt %, Fe_2O_3(T) is moderate relative to and MgO with mean value of 1.95 wt % and 0.02 wt % respectively. The mean P_2O_5 = 0.03 wt % and Mg#=0.46. However, the. Na_2O and K_2O contents in the rocks range from 3.37-4.36 wt % and 4.66-5.15 wt % respectively. Nevertheless, their TiO_2 and CaO content vary from 0.03-0.20 wt % and 0.06-0.17 wt % respectively. The A/CNK=1.23-1.39 and K_2O+Na_2O (NK) =8.09-9.02. Trace element content show a significant different from the biotite granite (Table 1) with LILE very low concentration of Ba (15-79 ppm), Rb (153-261 ppm), Sr (4-9 ppm) with one sample having moderate concentration in Ba (896 ppm) and Sr (346 ppm). Meanwhile, the HFSE show low Nb (8 ppm), Zr (533.5 ppm), Hf (4.3 ppm) and Ta (4.1 ppm), The LREE also show high values relative to the HREE with the ratios of $(La/Lu)_N$ = 3.66-49.10, $(Gd/Lu)_N$ = 0.51-4.79. They display a strong negative Eu anomaly with $(Eu/Eu^*)_N$ = 0.08-0.14, with one sample showing a strong positive anomaly (Figure 6). The Rb/Sr varied from 17.22-65.25, K/Rb from 163.6-252.94 and Sr/Y from 0.03-0.14 except for one sample with high Sr/Y ratio of 346.

5. Discussion

5.1.Fractional Crystallization

The geochemistry of the Somie-Ntem granitoids show characteristics that differentiate group I from II. Harker diagrams for both groups show a negative correlation to SiO_2 for all major elements including Ba and Sr except Na_2O and K_2O that show scattering (Figure 7). This indicates that the concentration of Na_2O and K_2O in the granitoids is independent of SiO_2 and characteristic of mineral fractionation. According to [39], the CaO, Fe_2O_3(T) and MgO contents increase in the early forming rocks with the fractionation of early forming minerals like amphiboles, biotite, plagioclase and decrease in those of the late phase [40]. This suggest that fractionation from a common melt or parent magma that began with the formation of group I rocks (Tn→GD→Gr) then ended with AGr of groups II [41]. However, the extreme depletion of Ba and Sr and the low CaO, MgO and TiO_2 content in the groups II rocks suggested a situation of retracted fractional crystallization [75]. Several authors have used the binary plot between incompatible and compatible trace and REE to test for the process of fractional crystallization in magmatic rocks. Harkerdiscriminative plots (Figure 8a, Figure 8b and Figure 8c) of [42,43,44,45] show that the group I rocks of the Somie-Ntem area originated from a common melt and differentiated into the different rock type through fractional crystallization. This let to high TiO_2 content in least fractionated rocks while the most fractionated are low in TiO_2 [46] controlled by k-feldspars, biotite and hornblende while plagioclase play a minor role [46,47]. However, the scattering along the linear line is most likely associates with crustal assimilation [48]. High LREE shown by the Somie-Ntem granitoid and the pronounced negative Nb, Ti and P anomalies suggests constant titanite and allanite fractionation in the magma while the moderate to slightly positive $(Eu/Eu^*)_N$ anomaly shown by the group I granitoids indicates either magma mixing [41] or variable accumulation and/or feldspars fractionation within a continuous melt [46]. Nevertheless, the strong negative $(Eu/Eu^*)_N$=0.08-0.14 shown by the group II rocks indicates the influence of plagioclase in the differentiation process. According to [49], negative Eu anomaly indicates a high removal of feldspars from a felsic melt through crystal fractionation or partial melting as well as enrichment of mafic mineral. Meanwhile, the deviation from the vertical trend shown by group II samples, suggests either a different source or highly fractionated magma and possible interference with post magmatic hydrothermal activity.

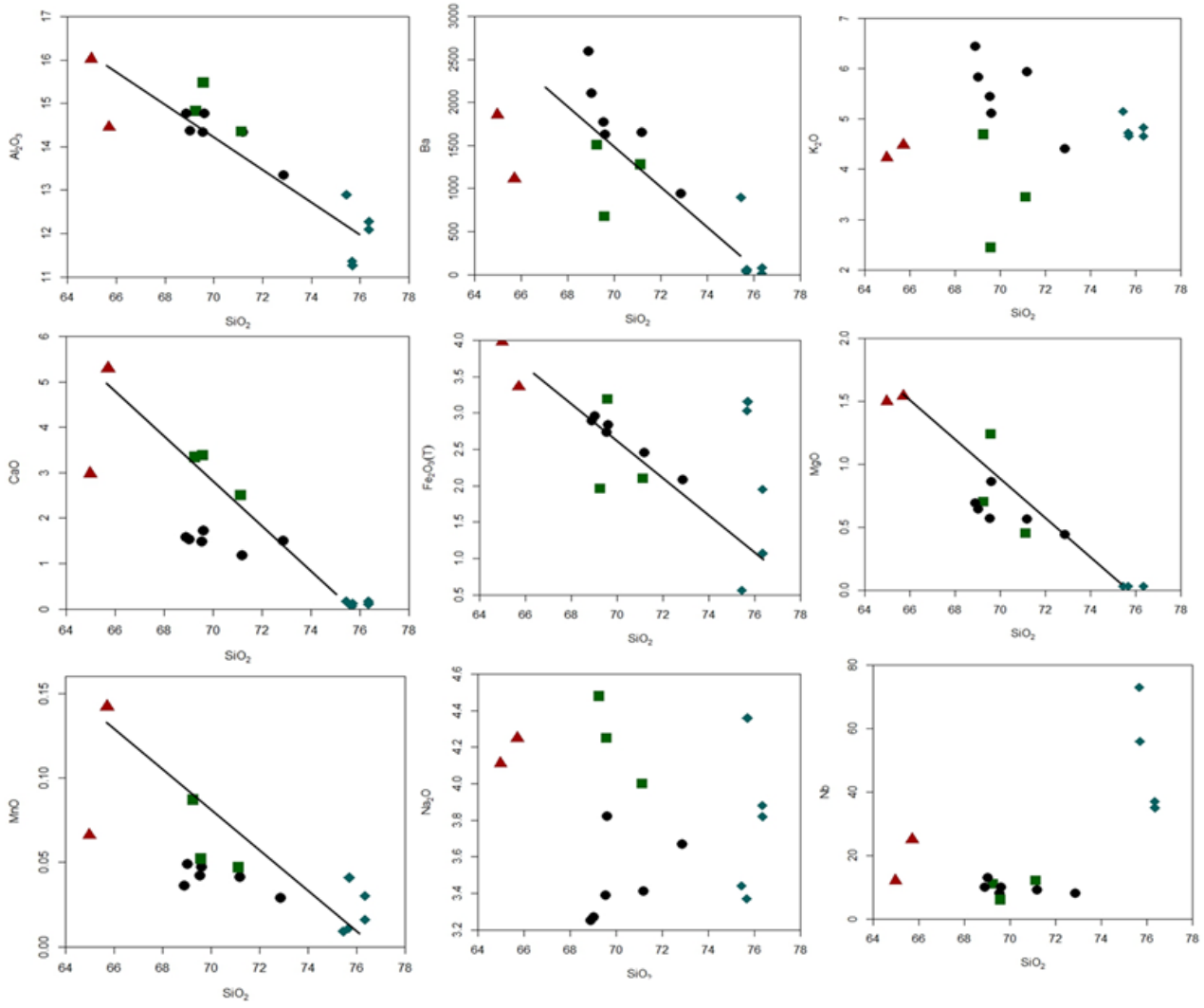

Figure 7. Hacker diagrams of selected major and trace elements for the Somie-Ntem granitoids

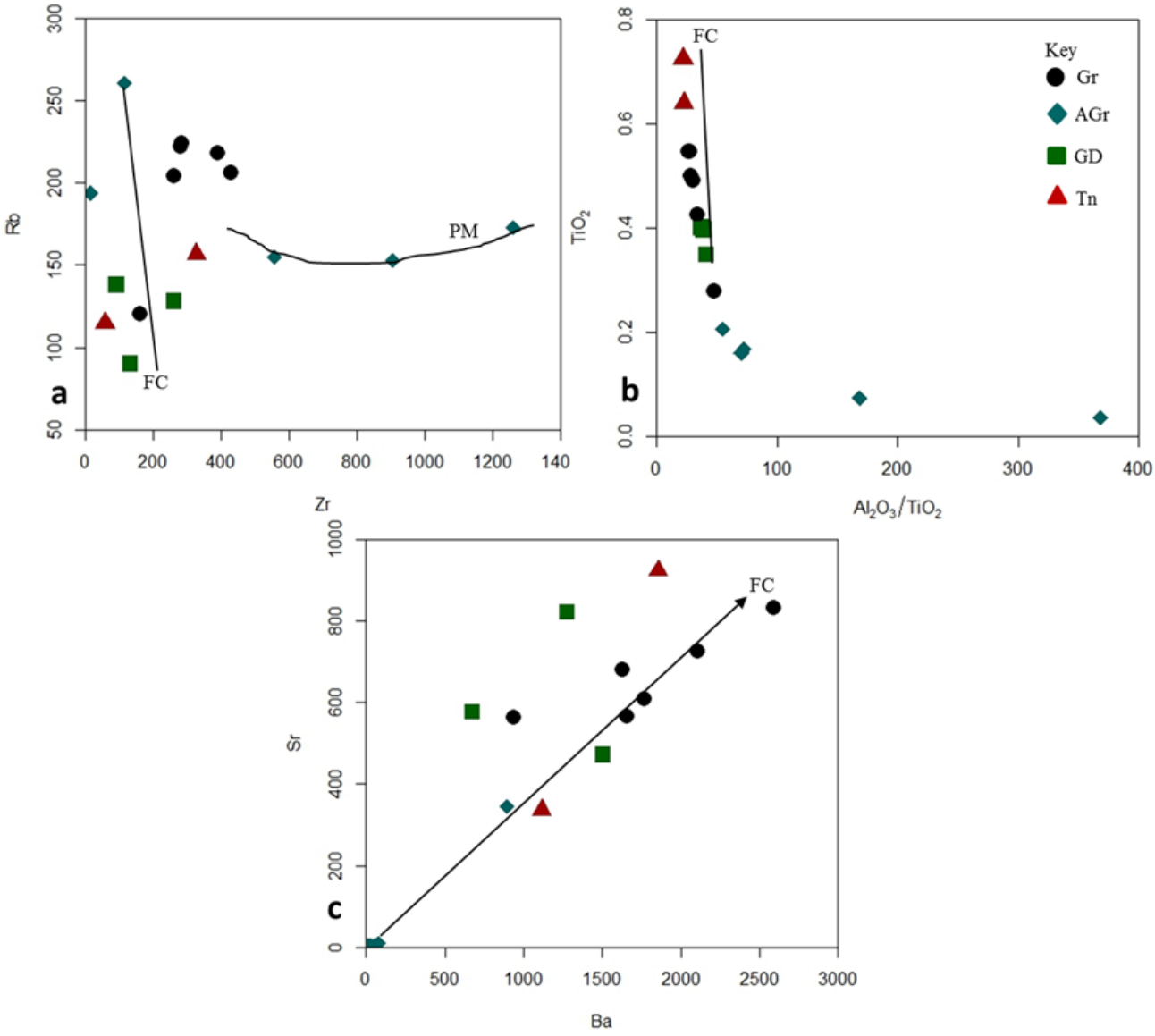

Figure 8. Discrimination diagrams showing the fractional crystallization (FC) and partial melting (PM) trends of the Somie-Ntem granitoids; a) Zr vs Rb [42]; b) Al_2O_3/TiO_2 vs TiO_2 [43] and c) Ba vs Sr [44,45].

5.2. Source and Tectonic Setting

The major elements composition show a high Na2O + K_2O (6.69-9.70 wt %), K_2O/Na_2O=0.5-1.74, and $Al_2O_3/(CaO+Na_2O+K_2O) \leq 1.1$ indicating K-rich granitoids with shoshonite and high calc-alkaline affinity, strongly metaluminous to weakly peraluminous and mainly of I-type granitoids. However, the AGrmetaluminous to weakly peraluminous rocks display strange geochemical characteristic that resembles anorogenic setting (Figure 9c). Experimental models on the origin of crustal rocks suggest that the appropriate sources for high-K, I-type granitoid magmas (AGr) is through partial melting of hydrous, calc-alkaline to high-K calc-alkaline, mafic to intermediate metamorphic rocks in the crust [50]. Partial melting from a plagioclase depleted source model is also supported by the pronounced negative anomaly $((Eu/Eu^*)_N$ =0.08-0.14) expressed by the group II granitoids [51]. Meanwhile, the rest of the granitoids show very weak negative to slightly positive Eu anomaly $((Eu/Eu^*)_N$=0.52-1.37) suggesting a very low degree of partial meting involving the fractionation of the felsic components in the melt [41,52]. Ref [53] also explained that such high-k-calc-alkaline rocks are mostly associated with post-collisional setting. Somie-Ntem granitoids show strong similarity to those of the Bamenda area [54] in terms of their Ba-Sr content and $(Eu/Eu^*)_N$ anomalies (Figure 10 and Figure 11). Group II rocks (Ba-Sr poor and negative Eu) plot within the post orogenic field (Figure 10b) [59] which is typical of intraplateleucogranites [62]. Meanwhile, Group I rocks (Ba-Sr rich) plot in the syn-to-post collisional fields similar to those of the Bamenda area [54]. The discrimination diagram of [55], plots these granitoids (group I) into volcanic arc and Syn-collisional environments (Figure 12) similar to most WCD Pan-African granitoids [40,56,57]. The group I rocks display LILE enrichment relative to the HFSE, negative Ti, Nb, P and positive Pb anomalies common with magma from supra-subduction environment and possible crustal contamination as the magma evolved [46]. Such subduction setting are often characterized by variable metasomatism [58] whereby, the subduction lithospheric plate preceded a process of collision setting during which dehydration of the subducted oceanic plate material

caused potassium metasomatism of the lithospheric mantle [15]. The scattering of the group I samples in the classification diagram (Figure 9) of [36] and [37] show that the magma either experience crustal contamination or modification during post magmatic deformation. On the other hand, the group II granitoids plots into the post orogenic field (Figure 10) which is very typical for leucocratic granitoids within the WCD [1]. Studies on granitoids of leucocratic composition within the Himalayas have shown a strong link with the regional shear zone wherein, shear movement forces magma to move from high strain compressional zones to that of low strain extension [60]. Based on that, the proximity of the Somie-Ntem area to the Tcholliré-Banyo fault in particular, and the CCSZ in general presents a suitable tectonic setting for emplacement of the group II leucocratic granitoids.Nevertheless, the post orogenic setting for group II rocks suggest partial melting of new material of intermediate composition added at the lower lithospheric crust [76].

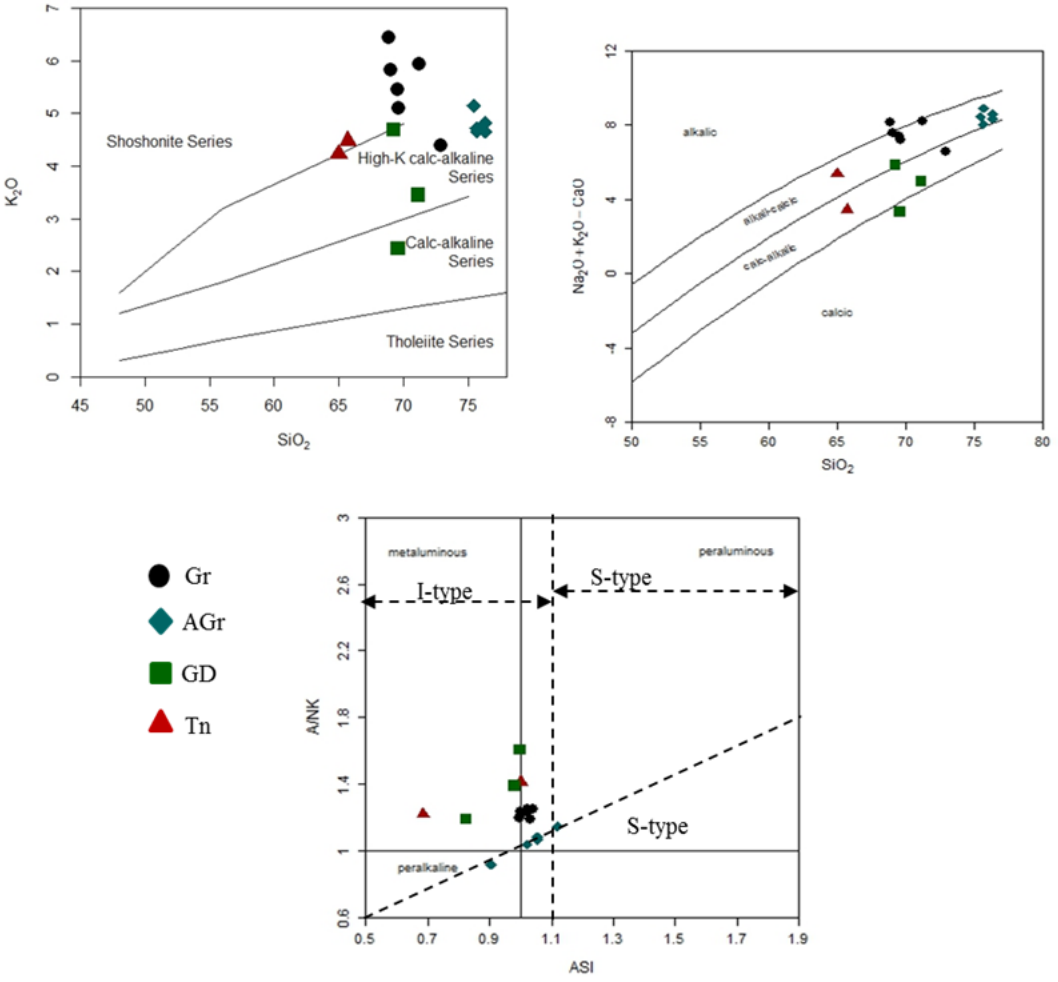

Figure 9. (a) K_2O vs SiO_2 diagram showing the limits of calc-alkaline and shoshonitic series by [37]; (b) Na_2O+K_2O-CaO vs SiO_2 and A/NK vs ASI diagrams of [36]. I and S-type boundary (dash line adopted from [74]

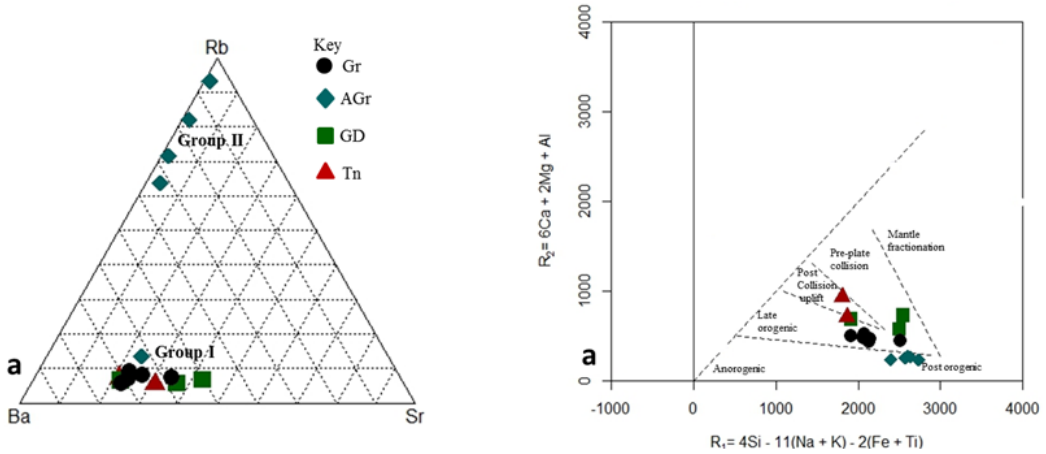

Figure 10. Discrimination diagrams for the Somie-Ntem granitoids, a) ternary diagram of Sr-Rb-Ba [61]; b) R_1-R_2millications diagram of [59] showing the tectonic setting of the two groups of granitoids.

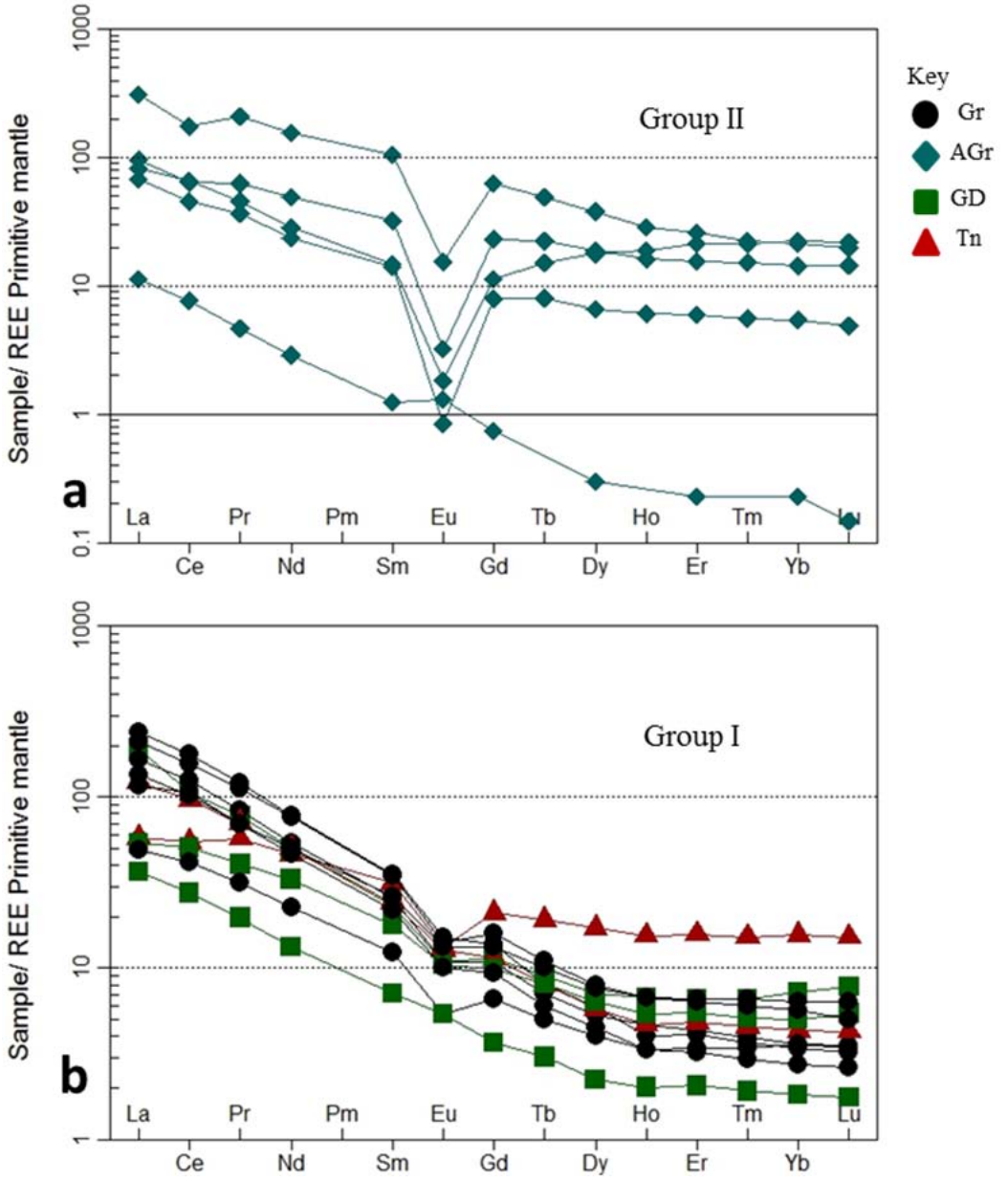

Figure 11. Spider plot showing the different behavior of the granitoids of a) Group II; b) Group I.

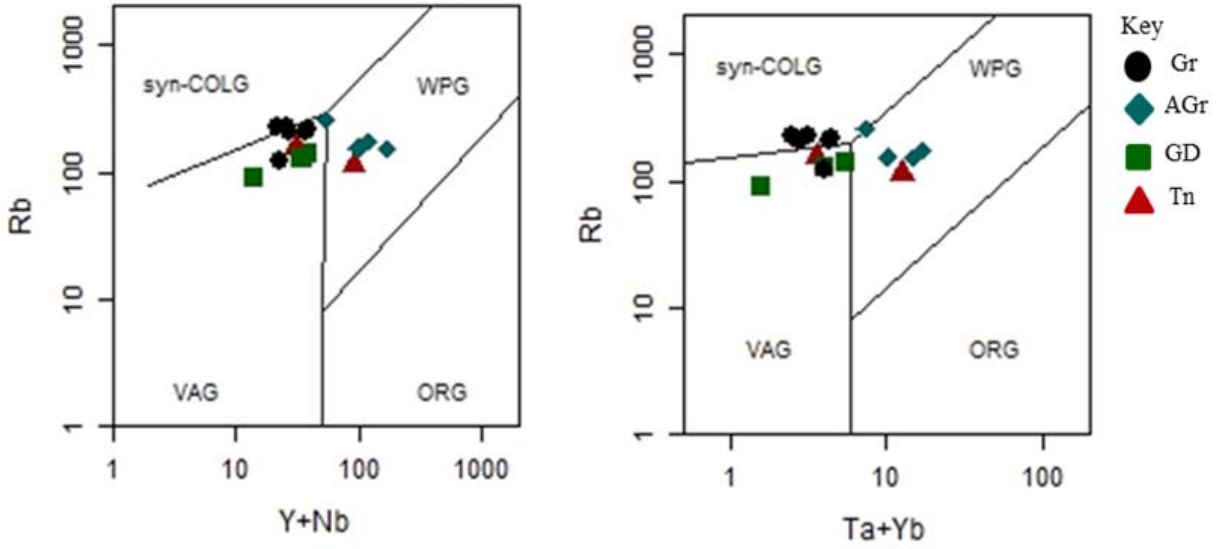

Figure 12. Tectonic discrimination diagrams for the Somie-Ntem segment granitoids of the Tikar plain after [55]

5.3. Implication to Pan-African Evolution

From petrography, the group II granitoids display leucocratic composition with very low mafic content andaintensemyrmekitic texture indicating the rocks suffered both magmatic and post magmatic lateration in the area [62,63]. From petrography, group II granitoids display leucocratic composition with intense granophyric texture indicating that the rocks suffered both liquid and solid state deformation [66,67]. Nevertheless, the trace elements spider plot [34,35] for both rock groups show a strong negative Nb, P and Ti anomalies (Figure 6) suggesting a possible process of crustal contamination of the magma during evolution [15,50,65]. The low ratio of Rb/Sr < 4 expressed by the group I rocks, suggest biotite precipitation during melting and the influx of vapor within the magmatic melt during evolution while the high ratio of >4 reflects melting that took place during dehydration process [65,66].

According to [67], the emplacement of Pan-African granitoid followed a period of prevailing compressional regime that involved the formation of subduction and arc granitic rocks. These characteristics suggest magma derived from calc-alkaline metaluminous to Peraluminous I-type sources, emplaced during compressional processes associated with subduction and arc granitic formations with a likely mantle influx [67,6] associated with the D_2 and D_3 deformation [19,69]. However, the high Rb/Sr ratio, HFSE with negative Eu $(EuEu^*)_N$=0.08-0.19), very low Ba/Rb and Sr/Y ratios rather indicates a magma source depleted of Ba and Sr and rich in Nb, Zr, Y, Rb intruded under extensional forces that occurred at within plate setting, corresponding to post orogenic regime [67], or a rapid tectonic transition from crustal thickening to thinning at subduction environment representing the final magmatic stage of an extensive arc system [70]. The Ba-Sr variation observed in this study is common with most granitic environments within the Cameroon mobile belt (e.g. [54]) and suggest an evolutionary history that spanned from early crustal shortening and thickening of the Pan-African, through conjugate wrench movement that was followed by advanced delamination of the lithosphericmantle into a widespread period of melting and granitization across the Cameroon mobile belt [71,72].

6. Conclusions

Petrography and geochemical data show for types of granitoids in the area including: Gr, GD AGr and Tn. However, these rocks show some distinct features that broadly classify them into two rock groups. Group I rocks having Gr, GD, and Tn compositions, contain mainly biotite and amphibole, rich in Ba-Sr, moderately negative to slightly positive Eu anomaly and are generally syn-collision and arc granitoids. Their emplacement relates to orogenic regime at subduction. Group II granitoids consist of AGr, leucocratic in composition, bearing pyroxene and amphibole and show a dense myrmekitic and granophyric textures. Their trace elements content show significant depletion in Ba-Sr, show strong negative Eu anomaly and strictly post orogenic. Source material for group II granitoids indicates partial melting from a plagioclase depleted source at the lower lithospheric crust.

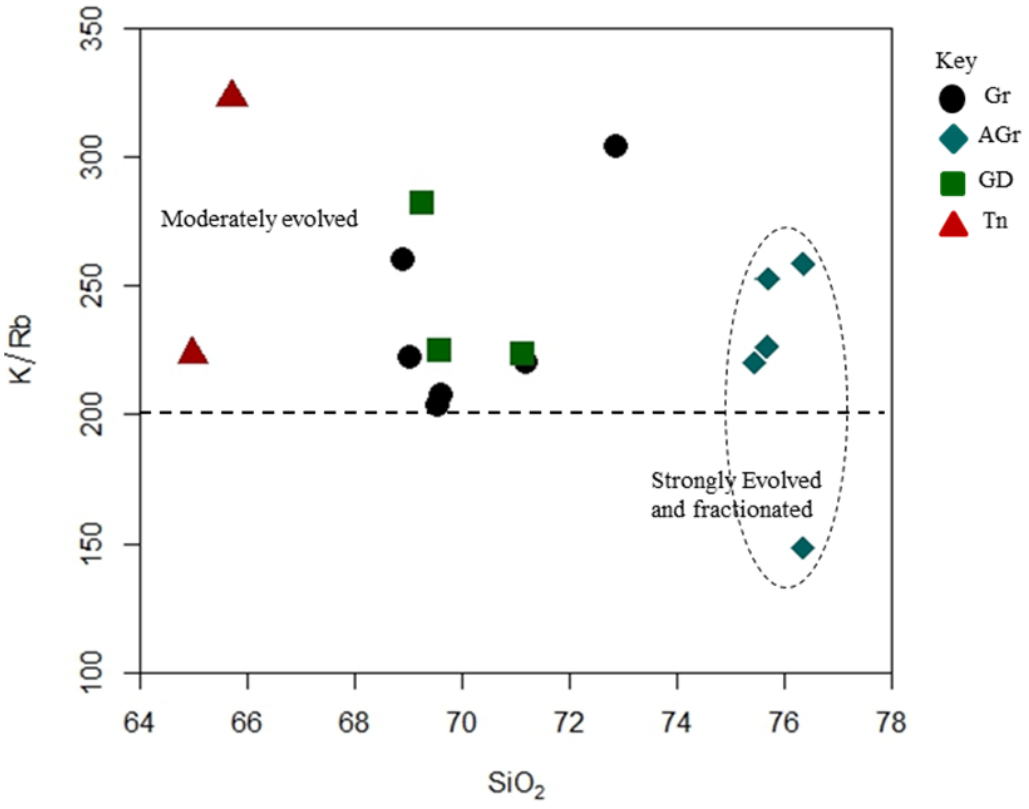

Figure 13. SiO_2 vs K/Rb diagram showing the evolution of the Somie-Ntem granitoids [64], Note dash circle representing the granitoids of mesocratic composition

Acknowledgments

The author appreciate the great financial assistance obtained during the field work of this project from the capacity building project in the mining sector of Cameroon (PRECASEM) under the Ministry of Mines Industries and Technological Development (MINMIDT).

References

[1] KouankapNono G. D., 1, Nzenti J. P. and Suh C. E. and Ganno S. (2010). Geochemistry of Ferriferous, High-K Calc-Alkaline Granitoids from the Banefo-MvoutsahaMassif (NE Bafoussam), Central Domain of the Pan-African Fold Belt, Cameroon. *The Open Geological Journal*, 4: 15-28.

[2] Ngako V., Jegouzo P. and Nzenti J. P. (1991). Le Cisaillement Centre Camerounais. Roˆ le structural et géodynamique dans l'orogenèse pan-africaine. *Comptesrendus De l'Académie des Sciences Paris*, 315: 457-463.

[3] Bella Nké B. E., Njanko T., Mamtani M. A., Njonfang E. and Rochette P. (2018). Kinematic evolution of the Mbakop Pan-African granitoids (western Cameroon domain): An integrated AMS and EBSD approach. *Journal of Structural Geology*, 111: 42-63.

[4] Toteu S. F., Van Schmus W. R., Penaye J. and Michard A. (2001). New U–Pb and Sm–Nd data from north-central Cameroon and the pre-Pan African history of central Africa. *Precambrian Research*, 108: 45-73.

[5] Njonfang E., Tchoneng G. T., Cozzupoli D. and Lucci F: (2013). Petrogenesis of the Sabongari alkaline complex, Cameroon line (central Africa): Preliminary petrological geochemical constraints. *Journal of African Earth Sciences*, 83: 25-50.

[6] Lasserre M. (1967). Données géochronologiques nouvelles acquises au 1er janvier 1967 par la méthode au strontium appliquée aux formations cristallines et cristallophylliennes au Cameroun. *Ann Faculté de Science Université Clermont-Ferrand Géologie et Minéral*, 36: 109-144.

[7] Tchameni R., Sun F., Dawaï D., Danra G. Tékoum L. NomoNegue E., Vanderhaeghe O. and Nzolang C. (2016). NguihdamaDagwaï-Zircon dating and mineralogy of the Mokong Pan-African magmatic epidote-bearing granite (North Cameroon). *International Journal of Earth Sciences (GeolRundsch)*, 105: 1811-1830.

[8] Lasserre M., Tempier P. and Soba D. (1981). Petrographie et geochronologie Rb/Sr des granites cambriens de Goutchoumi et d'Anloa (Cameroun). Bulletin de SociétéGéologique de la France 23: 511-514.

[9] Soba D., Michard A., Toteu S. F., Norman D. I., Penaye J., Ngako V., Nzenti J. P. and Dautel, D. (1991). Données géochronologiques nouvelles (Rb-Sr, U-Pb et Sm- Nd) sur la zone mobile panafricaine de l'Est-Cameroun: âge Protérozoïque supérieur de la série de Lom. *ComptesRendusAcadémie Sciences Paris*, 312: 1453-1458.

[10] Tchouankoue J. P. (1992). La syénite de Bangangté: un complexe panafricain à caractères in termediaires. Pétrologie-Géochimie. Thèse Doctorat 3è cycle, *Université de Yaoundé I*. p 160.

[11] Nguiessi T. C., Nzenti J. P., Nsifa E. N., Tempier P., Tchoua F.M. (1997). Les granitoïdes calco-alcalins, syncisaillement de Bandja dans la chaîne panafricaine nord-équatoriale au Cameroun. C. R. *Academic of Sciences Paris*, 325: 95-101.

[12] Tagne-Kamga G. (2003). Petrogenesis of the Neoproterozoic Ngondo plutonic complex (Cameroon, west central Africa): a case of late-collisional ferro-potassicmagmatism. *Journal of African Earth Sciences*, 36: 149-171.

[13] Nzolang C., Kagami H., Nzenti J. P., Holtz F. (2003). Geochemistry and preliminary Sr-Nd isotopic data on the Neoproterozoic granitoids from the Bantoum area, West Cameroon: evidence for a derivation from a Paleoproterozoic Archean crust. *Polar Geosciences*, 16: 196-226.

[14] Tetsopgang S. (2003). Petrology, geochemistry and geochronology of Pan-African granitoids in the Nkambé area, Northwestern Cameroon, Africa. PhD Thesis, *Nagoya University, Japan.*

[15] Djouka-Fonkwé M. L., Schulz B., Schüssler U., Tchouankoué J. P. and Nzolang C. (2008). Geochemistry of the Bafoussam Pan-African I and S- type granitoids in western Cameroon. *Journal of African Earth Sciences*, 50: 148-167.

[16] Nzina A. C., Nzenti1 J. P., Njiosseu. E. L. T., Ganno S. and Ngnotue T. (2010). Synkinematicferro-potassicmagmatism from the Mekwene-NjimafofireFoumban Massif, along the Foumban-Banyo shear zone in central domain of Cameroon Pan-African fold belt. *Journal of Geology and Mining Research*. 2: 142-158.

[17] Njonfang E. and Moreau M. (2000). The mafic mineralogy of the Pandé massif, Tikar plain, Cameroon: Implications for a peralkaline affinity and emplacement from highly evolved alkaline magma. *Mineralogical Magazine*, 64: 525-537.

[18] Castaing C, Feybesse J. L., Thiéblemont D., Triboulet C. and Chèvremont P. (1994). Palaeogeographical reconstructions of the Pan-African/Brasilianoorogen: closure of an oceanic domain or intracontinental convergence between major blocks? *Precambian Research*, 69: 327-344.

[19] Toteu S. F., Penaye J. and PoudjomDjomani Y. (2004). Geodynamic evolution of the Pan-African belt in central Africa with special reference to Cameroon. *Canadian Journal of Earth Sciences*, 41: 73-85.

[20] Tchameni R., Pouclet A., Penaye J., Ganwa A. A. and Toteu S. F. (2006). Petrography and geochemistry of the Ngaoundéré Pan-African granitoids in Central North Cameroon: Implications for their sources and geological setting. Journal of African Earth Sciences, 44: 543-560.

[21] Djouka-Fonkwe´ M. L. (2005). Association of S-type and I-type granitoids in the Neoproterozoic Cameroon orogenic belt, Bafoussam area, west Cameroon: geology, geochemistry and petrogenesis. *Unpublished PhD Thesis*, University of Wu¨rzburg, Germany, p197.

[22] Abdelsalam M. G., Liégeois J. P. and Stern R. J. (2002). The Saharan meta-craton. *Journal of African Earth Sciences*, 34: 119-136.

[23] Affaton P. (1990). Le bassin des Volta (Afrique de l'Ouest) : une marge passive d'âge protérozoïque supérieur, tectonisée au panafricain (600 ± 50 Ma). *Etudes etThèses ORSTOM*, Paris, France.

[24] Caby R. and Boessé J. M. (2001). Pan-African nappe system in southwest Nigeria: the Ife-Ilesha schist belt. *Journal of African Earth Sciences*, 33: 211-225.

[25] Nguiessi-Tchankam C. and Vialette, Y. (1994). Donne´esge´ochronologiques (Rb-Sr, Pb-Pb, U-Pb) sur le complexe plutonique de Bandja (Centre Ouest Cameroun). *ComptesRendus de l'Acade´mie des Sciences Paris*, 319: 317-324.

[26] Jacquemin H., Sheppard S. M. F. and Vidal P. (1982). Isotopic geochemistry (O, Sr, Pb) of the Golda Zuelva and Mboutouanorogenic complexes, North Cameroon: mantle origin with evidence of crustal contamination. *Earth and Planetary Science Letters*, 61: 97-111.

[27] Parsons I., Brown W. L. and Jacquemin H. (1986). Mineral chemistry and crystallization conditions of the Mboutou layered gabbro-syenite-granite complex, North Cameroon. *Journal of Petrology*, 27: 1305-1329.

[28] Ngounouno I., Moreau C., Déruelle B., Demaiffe D. and Montigny R. (2001). Pétrologie du complexe alcalin sous-saturé de Kokoumi (Cameroun). *Bulletin de la SociétéGéologique de France* 172: 675-686.

[29] Bella Nké B. E., Njanko T., Kwékam M., Njonfang E., Naba S., Tcheumenak K. J., Gountié M., Rochette P. and Nédélec A. (2014). Structural study of the Foréké-Dschang trachytic dome (Mount Bambouto, West Cameroon): An anisotropy of magnetic susceptibility (AMS) approach. *Journal of African Earth Sciences*, 95: 63-76.

[30] Njonfang E., Nono A., Kamgang P., Ngako v. and Tchoua F. M. (2011). Cameroon line alkaline magmatism (Central Afirca): A reappraisal. *The geological Society of America*, 478: 173-191.

[31] Njonfang E., Moreau C. and Tchoua F. M. (1998). La bande mylonitique Foumban - Bankim, Ouest Cameroun. Une zone de cisaillement de haute température. C. R. *Academic Science. Paris*327: 735-741.

[32] Njonfang E., Ngako V., Kwékam M. and Affaton P. (2006). Les orthogneisscalco-alcalins de Foumban-Bankim: témoins d'une zone interne de marge active panafricaine en cisaillement. C. R. *Geosciences*. 338: 606-616.

[33] De La Roche H., Leterrier J., Grandclaude P. and Marchal, M. (1980). A classification of volcanic and plutonic rocks using R1R2-diagram and major element analyses, its relationships with current nomenclature. Chemical Geology 29, 183-210.

[34] McDonough W. F. and Sun S. S. (1995). The composition of the Earth. *Chemical Geology*, 120: 223-253.

[35] Sun S. S. and McDonough W. F. (1989): Chemical and isotopic systematics of oceanic basalts: implications for mantle composition and processes. In: Saunders, A. D., M.. J.(Eds.), Magmatism in ocean basins, vol. 42. Geological Society of London Special Publication, p 429-448

[36] Frost B. R., Barnes C. G., Collins W. J., Arculus R. J., Ellis D. J. and Frost C. D. (2001). A geochemical classification for granitic rocks. *Journal of Petrology*. 42: 2033-2048.

[37] Peccerillo A. and Taylor, S. R. (1976). Geochemistry of Eocene calc-alkaline volcanic rocks from the Kastamonu area, Northern Turkey. *Contributions to Mineralogy and Petrology*, 58: 63-81.

[38] Le Marechal A. (1975). Carte géologique de l'Ouest du Cameroun et de l'Adamaoua. Office de la Recherche Scientifique et Technique Outre-Mer (ORSTOM), Service Central de documentation, 70-74, *Route d'Aulnay-93 Bondy France*.

[39] Imeokparia E. G. (1981). Ba/Rb and Rb/Sr ratios as indicators of magmatic fractionation, postmagmatic alteration and mineralization Afu Younger Granite Complex, Northern Nigeria. Geochemical Journal, 15: 209-219.

[40] Hassanen M. A., Egnisr S. A. and Mohamed F. H. (1996). Geocheinistry and petrogenesis of Pan-African I-type granitoids at GabalIglaAhmar, Eastern Desert, Egypt. *Journal of African Earth Sciences*, 22: 29-42.

[41] Kwékam M., Hartmann G., Njanko T., Tcheumenak K. J., Fozing E. M., Njonfang E. (2015). Geochemical and Isotope Sr-Nd Character of Dschang Biotite Granite: Implications for the Pan-African Continental Crust Evolution in West-Cameroon (Central Africa). *Earth Science Research*; 4: 88-102.

[42] Martin H. (1987): Petrogenesis of Archaeantrondhjemites, tonalites, and granodiorites from eastern Finland: major and trace element geochemistry. Journal of Petrology, 28: 921-953.

[43] Sun S. S. and Nesbitt R. W. (1978): Geochemical irregularities and genetic significance of ophiolitic basalts. Geology, 6: 689-693.

[44] Wilson, M., (1989): Igneous Petrogenesis. Unwin Hyman, London.

[45] Hanson G. N. (1978): The application of trace elements to the petrogenesis of igneous rocks of granitic composition. Earth and Planetary Science Letters, 38: 26-43.

[46] Nascimento R. S. C., Mcreath I. and Galindo A, C. (2010). Relationships between Shearing and Granitic Magma Emplacement: the Remígio-Pocinhos Shear Zone in the São José do Campestre Massif, NE Brazil. *Geologia USP-SerieCientifica*, 3: 3-18.

[47] Janoušek V. Bowes D. R., Rogers G., Farrow C. M and Jelinek E. (2000): Modelling diverse processes in the petrogenesis of a composite batholith: the Central Bohemian Pluton, Central European Hercynides. Journal of Petrology, 41: 511-543.

[48] Motoki A., Sichel S. E., Vargas T., Melo D. P. and Motoki K. F. (2015): Geochemical behaviour of trace elements during fractional crystallization and crustal assimilation of the felsic alkaline magmas of the state of Rio de Janeiro, Brazil. Anais da Academia Brasileira de Ciências, 87: 1959-1979.

[49] Rollinson H. R. (1993). Using geochemical data: evaluation, presentation, interpretation: Longman Group, p352.

[50] Roberts M. P. and Clemens J. D. (1993). "Origin of high-potassium, calcalkaline, I-type granitoids". *Geology*, 21: 825-828.

[51] Térakado Y. and Masuda A. (1988). Trace element variations in acidic rocks from the inner zone of southwest Japan. *Chemical Geology*, 67: 227-241.

[52] El-Afandy A. H., AlrahmanEmbaby A. B. D. and. El Harairey M. A. (2015). Geology, geochemistry and radioactivity of granitoid rocks of Abu Marw area, South Eastern Desert, Egypt. *Nuclear Sciences Scientific Journal*, 4: 61-83.

[53] Liégeois J. P., Navez J., Hertogen J. and Black R. (1998). Contrasting origin of post-collisional high-K calc-alkaline and shoshonitic versus alkaline and peralkaline granitoids: the use of sliding normalization. *Lithos*, 45: 1-28.

[54] KouankapNono G. D., Wotchoko P., Magha A., Ganno S., Njoya N., Ngambu A. A., Jean Paul Nzenti J. P. and Kabeyene V. K. (2018). Contrasting Ba-Sr Granitoids from Bamenda Area, NW Cameroon: Sources Characteristics and Implications for the Evolution of the Pan African Fold Belt. *Journal of Geosciences and Geomatics*, 6: 65-76.

[55] Pearce J. A., Harris N. B. W., and Tindle A.G. (1984). "Trace elements discrimination diagrams for the geotectonic interpretation of granite rocks". *Journal of Petrology*, 25: 956-983.

[56] El Baghdadi M., El Boukhari A., Jouider A., Benyoucef A. and Nadem S. (2003). Calc-alkaline Arc I-type Granitoid Associated with S-type Granite in the Pan-African Belt of Eastern Anti-Atlas (Saghro and Ougnat, South Morocco). *Gondwana Research*, 6: 557-572.

[57] Asran M. A. and Ezzat M. R. (2012). The Pan-African calc-alkaline granitoids and the associated mafic microgranular enclaves (MME) around the Wadi Abu Zawal North Eastern Desert, Egypt: Geology, Geochemistry and Pretrogenesis. *Journal of Biology and Earth Sciences*, 2: 1-16.

[58] Harlov D. E. and Austrheim H. (2013). Metasomatism and the Chemical Transformation of Rock: Rock-Mineral-Fluid Interaction in Terrestrial and Extraterrestrial Environments, *Earth System Sciences*, p16.

[59] Batchelor R. A. and Bowden P. (1985). Petrogenetic interpretation of granitoid rocks series using multicationic parameters. *Chemical Geology* 48: 43-55.

[60] Nabelek P. I. and Liu M. (2004). Petrologic and thermal constraints on the origin of leucogranites in collisional orogens. *Earth and Environmental Science and environment Transactions of the Royal Society of Edinburgh*, 95: 73-85.

[61] Karimpour M. H. and Bowes W. W. (1983): Application of trace elemnts and isotopes for discriminatig between porphyry molybdenum, copper, and tin systems and the implications for predicting the grade: Global Tectonics and Metallogeny, 2: 29-36.

[62] Barker S. D. (2007). Compositions of granophyre, myrmekite and graphic granite: *Geological Society of America Bulletin*, 81: 3339-3350.

[63] Fozing E. M., Kwékam M., Njanko T., Njonfang E., Séta N., Yakeu S. A. F. and Sawadogo S. (2014): Structural evolution of the Pan-African Misajé pluton (Northwestern Cameroon). Syllabus Review, 5: 12-26.

[64] Blevin P. (2003). Metallogeny of granitic rocks. In: Magmas to mineralization. Blevin P. et al. (eds). The Ishihara symposium: p1-4.

[65] Chebeu C., Nlend C. D. N., Nzenti J. P. and Ganno S. (2011). Neoproterozoic high-K Calc-alkaline Granitoids from Bapa-Batié, North Equatorial Fold Belt, Central Cameroon: Petrogenesis and Geodynamic Significance. *The Open Geology Journal*, 5: 1-20.

[66] Harrisson T. M., Grove M., McKeegan K. D., Coath C. D., Lovera O. M and Le Fort P. (1999). "Origin and episodic emplacement of the Manaslu intrusive complex, central Himalaya", *Journal of. Petrology*, 40: 3-19.

[67] El-Mettwaly A. A., Zalata A. A. and Abu El-Enen M. M. (1992). The evolution of the Pan-African granitoid rocks: geochemical evidences from SW Sinai massif, Egypt. *Journal of African Earth Sciences(and the Middle East)*, 14: 111-119.

[68] Eby N. (2014). A-type granites: characteristics, petrogenesis and their contribution to the growth of the continental crust. *University of Massachusetts, Lowell*, MA 01854, USA.

[69] Toteu S. F., Macaudière J., Bertrand J. M., Dautel D. (1999). Metamorphic zircon from North Cameroon; implications for the Pan-African evolution of central Africa. *GeologischeRundschau*, 79: 777-788.

[70] Gehad M. S. (2000). Pan-African Younger Granitoids of the Southern Eastern Desert, Egypt: Geology, Geochemical Constraints, and Mineralization. *International Geology Review*, 48: 360-381.

[71] Toteu S. F. (1990): Geochemical characterization of the main petrographycal and structural units of northern Cameroon: implications for Pan-African evolution. Journal of African Earth Sciiences, 10: 615-624.

[72] Ngako V., Affaton P., Nnange J. M. &Njanko T. H. (2003). Pan-African tectonic evolution in the central and southern Cameroon: trans-pression and trans-tension during sinistral shear movements. *Journal of African Earth Sciences*, 36: 207-214.

[73] TchaptchetTchato D., Nzenti J. P., Njiosseu E. L., Ngnotue, T. and Ganno S. (2009). (Neoproterozoic metamorphic events in the Kekem area Central Domain of the Cameroon north equatorial fold belt): P-T data. *Journal of the Cameroon Academy of Sciences*, 8: 91-106.

[74] Chappell B.W. and White A. J. R. (1992). I and S-type granites in the Lachlan Fold Belt. Transactions of the Royal Society of Edinburgh: *Earth Sciences* 83: 1-26.

[75] Noble D. C., Haffty J. and Hedge C. E. (1969). Strontium and magnesium contents of some natural peralkaline silicic glasses and their petrogenetic significance. *American Journal of Science*, 267: 598-608.

[76] Rogers J. J. W. and Greengerg J. K. (1990): Late-orogenic, post-orogenic and anorogenic granites: Distinction by major element and trace element chemistry and possible origin. Jornal of Geology, 98: 291-309.